



HAL
open science

How complex is the time-averaged geomagnetic field over the past 5 Myr?

Julie Carlut, Vincent Courtillot

► **To cite this version:**

Julie Carlut, Vincent Courtillot. How complex is the time-averaged geomagnetic field over the past 5 Myr?. *Geophysical Journal International*, 1998, 134 (2), pp.527-544. 10.1046/j.1365-246x.1998.00577.x . insu-01570627

HAL Id: insu-01570627

<https://insu.hal.science/insu-01570627>

Submitted on 31 Jul 2017

HAL is a multi-disciplinary open access archive for the deposit and dissemination of scientific research documents, whether they are published or not. The documents may come from teaching and research institutions in France or abroad, or from public or private research centers.

L'archive ouverte pluridisciplinaire **HAL**, est destinée au dépôt et à la diffusion de documents scientifiques de niveau recherche, publiés ou non, émanant des établissements d'enseignement et de recherche français ou étrangers, des laboratoires publics ou privés.

How complex is the time-averaged geomagnetic field over the past 5 Myr?

Julie Carlut and Vincent Courtillot

Laboratoire de Paléomagnétisme, UMR CNRS 7577, Institut de Physique du Globe de Paris et Université Paris VII—Denis Diderot, 4 Place Jussieu, 75252 Paris Cedex 05, France

Accepted 1998 March 13. Received 1998 March 13; in original form 1997 February 10

SUMMARY

A basic tenet of palaeomagnetism is that the Earth's magnetic field behaves on average like that of a central axial dipole (g_1^0). Nevertheless, the question of possible persistent second-order features is still open. Recently Johnson & Constable (1995, 1996) performed a regularized non-linear inversion and found evidence for persistent non-zonal features. Formal uncertainties would indicate that there are significant (non-zero) terms at least up to degree and order 4. Using a recent compilation of two different data sets from lavas (0 to 5 Ma) and the Johnson & Constable codes, we test the robustness of this result. The data set has been divided into three subsets: the Brunhes polarity data (B), all normal polarity data (N) and all reverse data (R). In each subset of data, a prominent g_2^0 , of the order of 5 per cent of g_1^0 , is clearly present, as previously established by several authors. In some subsets, smaller terms appear: g_2^2 and g_1^1 in the Brunhes data, h_3^1 and h_2^1 in N, and h_2^1 , g_3^0 and g_3^3 in R. A threshold under which terms resulting from the inversion cannot yet be considered as robust appears to be of the order of 300 nT. Indeed, tests show that many terms, which are different for each epoch (B, N or R), may be artefacts due to aliasing because of poor site distribution, or due to the underestimation of *a priori* errors in the data; these could result from undetected tectonic rotations, non-horizontal palaeoslopes, or viscous overprints. Because of these limitations in resolution, it may not yet be possible to identify robustly terms other than the axial dipole and quadrupole. The persistence of high-latitude flux concentrations, hemispheric asymmetry or normal versus reversed field asymmetry cannot yet be considered as demonstrated.

Key words: geomagnetic field, inverse problem, palaeomagnetism, spherical harmonics.

1 INTRODUCTION

'When averaged over a sufficiently long time, the Earth's magnetic field reduces to that of an axial dipole aligned with the axis of rotation.' This statement has been the 'credo' of most palaeomagnetists for the last half-century and a fundamental basis for the success of plate-tectonic reconstructions. But the Earth's present field does not reduce to that of an axial dipole, and all of its components fluctuate with time. The larger internal part of these fluctuations, with time constants ranging from a year to hundreds of millions of years, is known as secular (or palaeosecular) variation (e.g. Courtillot & Valet 1995). As one jumps over timescales, from those of historical times (accessible to direct observation) to those of archaeomagnetism and palaeomagnetism (in which one must resort to fossil magnetization of artefacts and natural rocks), the question arises as to which features found on the shorter timescales might persist on the longer ones. The power spectrum

of the present geomagnetic field appears to be rather flat when continued downwards at the core–mantle boundary (e.g. Hulot & Le Mouél 1994). Although the axial dipole seems to stand above other terms (that is, the equatorial dipole and higher-order multipoles), some authors have assumed that this might be a transient feature. In any case, significant higher-order terms, including non-zonal ones, are present. In a compilation of historical measurements, Bloxham & Gubbins (1985) (see also Bloxham & Jackson 1992) find that two sets of higher-latitude flux concentrations, which might represent the traces of convective columns in the liquid core, tangential to its inner solid part, have persisted for three centuries. Should such features have persisted over the much longer periods accessible to archaeo- and palaeomagnetism, they might indicate control of the field by thermal anomalies in the deeper mantle (e.g. Gubbins & Kelly 1993). The fluid core is not expected to have a memory in excess of a few hundred to a few thousand years. For instance, Hulot & Le Mouél (1994) have shown that the

typical correlation times for all harmonic terms with degree larger than 1 were less than 300 years. In other words, the non-axial-dipolar part of the field is not necessarily expected to retain persistent features for longer times: some of the features found in the 300 years of historical data might therefore have appeared only a short time prior to the period over which these data are available.

In order to test this, palaeomagnetists have assembled data sets of remanent directions found in both lava and sediments for the past few million years. This duration was selected because it was expected to be long enough for the averaging of transient patterns, yet short enough that relative plate motions could be neglected. In this respect, we can mention the first significant data set (Lee 1983), in which 2244 palaeomagnetic directions from lava flows coming from 65 distinct sampling sites and spanning the past 5 Myr were assembled. [Note: in this paper, we do not use palaeointensities, which are much more difficult to determine, are still fraught with major uncertainties and are still quite few in number (see Kono & Tanaka 1995a)]. Though not formally published, the Lee data set has served as a basis for the statistical analyses of Merrill & McElhinny (1983) and many others that followed.

There are some fundamental differences between data coming from volcanic rocks and those from sediments. Magnetization in lava flows is a thermal remanence, and one expects that the component isolated after magnetic or thermal cleaning in the laboratory is an uncontaminated estimate of a quasi-instantaneous recording of the field direction: indeed, the cooling times for commonly encountered lava flows are on the order of days to months. The main difficulty is assigning an accurate age to the lava, and estimating properly the duration between successive lava flows. Volcanic processes tend to be highly irregular, and sequences of flows may either have recorded only a short interval of time or, on the other hand, be separated by very long gaps. The dispersion of magnetization directions is often considered to be a good index to distinguish between these various situations. On the other hand, sedimentary rocks will generally have averaged out some of the secular variation due to the very nature and duration of the isothermal recording process. Usual sedimentation rates imply that the amount of time represented in a single specimen may be of the order of hundreds to tens of thousands of years. This is why most detailed studies of secular variation rely primarily on volcanic rocks.

A notable exception, attempting to integrate also the information contained in the sedimentary record, is that of Gubbins & Kelly (1993). Gubbins & Kelly limited themselves to the past 2.5 Myr, combining full directional data (that is, both declination and inclination) from lava with inclination-only data from sediments. These were then inverted (the inversion being non-linear) to yield the mean-field structure for either the most recent normal (Brunhes) chron, i.e. the past 780 kyr, or all the normal (respectively, reverse) data for the whole 2.5 Myr period. The inverted mean field that they found bears some resemblance to the historical field: when the rather coarse and irregular site distribution is taken into account, two rotation-axis-parallel rolls seem to stand out, particularly in the Northern Hemisphere, which has denser data. A conclusion of Gubbins & Kelly's (1993) analysis was that the long-term average of the geomagnetic field does involve significant non-axial-dipolar features, in particular non-zonal ones, up to at least degree 4.

Two more recent attempts have led to more complete and documented volcanic data sets spanning the past 5 Myr (data set Q94—Quidelleur *et al.* 1994; and data set JC96—Johnson & Constable 1996). The Q94 data set comprises 3179 data from 86 distinct sites, whereas JC96 comprises 2187 records from 104 distinct locations (due to slightly different original data and selection criteria; see the respective papers for more information on this). JC96 was subjected to regularized non-linear inversion by Johnson & Constable (1995). We consider this to be the most complete and careful attempt at generating a mean-field model. Johnson & Constable (1995) performed the inversion up to degree and order 10, and presented tables of resulting coefficients up to degree and order 4. Most of these coefficients have amplitudes larger than the associated formal uncertainties, thus apparently confirming that the long-term field has a complex structure. Some traces of the rolls found by Gubbins & Kelly (1993) are still visible, although they appear to be very significantly attenuated. Also, a jack-knife approach shows that they depend largely on a rather limited number of sites. When data from these sites are eliminated, a smoother model with almost no roll structure is produced (Johnson & Constable 1995, Figs 13–15). Yet, many higher-order spherical harmonic terms, both zonal and non-zonal, still appear to be significant.

Following detailed analysis of inconsistent data from nearby sites, maximum number of spherical harmonic degrees sought in the inversion, influence of starting model and subset of data, Johnson & Constable (1995) concluded that non-zonal structure was a robust requirement in all their models. They also found that normal polarity models were incompatible with reverse polarity data, supporting previous claims that normal and reverse polarity field structures are significantly different. Such inferences have far-reaching implications for field generation models, and confirmation by independent groups is important. The aim of the present study is therefore to explore the significance of these models and their statistical robustness to a number of parameter and data changes. We attempt in particular to probe the influence of certain sites, of observational or experimental uncertainties, and of the data set itself, comparing results obtained with the two main data sets available, Q94 and JC96. Development of this work was first reported by Carlut & Courtillot (1995) (see also Carlut & Courtillot 1996), and this paper summarizes our main findings. Two contributions that appeared or were submitted after ours was first submitted (Kelly & Gubbins 1997; Johnson & Constable 1997) are addressed in a note added in proof at the end of this paper.

2 THE INVERSION PROCEDURE OF JOHNSON AND CONSTABLE

We followed the method proposed by Johnson & Constable (1995, hereafter JC95), using their original code (kindly made available to us). We will briefly recall the outline of their method. The mean field is supposed to derive from an internal harmonic potential, written in spherical coordinates in the usual way:

$$V(r, \theta, \varphi) = a \sum_{l=1}^N \left(\frac{a}{r} \right)^{l+1} \sum_{m=0}^l (g_l^m \cos m\varphi + h_l^m \sin m\varphi) P_l^m(\cos \theta), \quad (1)$$

where a is the Earth's radius, (r, θ, φ) are the spherical coordinates of radius, colatitude and longitude, and P_l^m are Schmidt partially normalized Legendre polynomials. The unknowns are the mean values of the Gauss (or spherical harmonic) coefficients g_l^m and h_l^m . These are related in a non-linear way to the observables, declination D and inclination I :

$$\mathbf{B} = -\nabla V$$

and

$$D = \tan^{-1}(-B_\varphi/B_\theta), \quad I = \tan^{-1}[-B_r/(B_\theta^2 + B_\varphi^2)^{1/2}]. \quad (2)$$

2.1 Generating regularized field models

JC95 give a detailed description of how they generate regularized field models. Observations (i.e. some form of mean values \bar{D} and \bar{I} , to be discussed further below) are related to the unknown spherical harmonic coefficients g_l^m and h_l^m through the non-linear equations summarized in eqs (1) and (2), with uncertainties σ_D and σ_I . A functional of the unknowns is minimized. This functional (eq. 10 in JC95) contains three components: the misfit of the model to the data, weighted by the inverses of their uncertainties; a tolerance level; and a regularization constraint. The idea is to construct a field model that is spatially smooth at the core surface and yet fits the observations to within the tolerance level. The regularization constraint consists of minimizing the root mean square (rms) value of either the radial field or its spatial gradient at the core-mantle boundary (CMB). The tolerance level is chosen to be consistent with the 95 per cent confidence limits on the expected value (χ^2 assuming that the data uncertainties are independent, zero-mean, Gaussian variables). A Lagrange multiplier describes the trade-off between the regularization constraint and the requirement that the data are fitted to within the tolerance level.

2.2 Linearization and inversion

The problem is linearized about a starting model and iterations are performed using the Occam algorithm of Constable, Parker & Constable (1987). Iterations are stopped when the minimum misfit becomes less than the tolerance level. The roughness of the inverted model can be followed as the iteration proceeds. Note that there is a misprint in eq. (B13) of Appendix B of JC95, which should read

$$\frac{\partial \beta}{\partial g_l^m} = \frac{B_r}{(B_\theta^2 + B_\varphi^2)^{3/2}} \left(B_\theta \frac{\partial B_\theta}{\partial g_l^m} + B_\varphi \frac{\partial B_\varphi}{\partial g_l^m} - \frac{(B_\theta^2 + B_\varphi^2)}{B_r} \frac{\partial B_r}{\partial g_l^m} \right). \quad (3)$$

2.3 Data uncertainties

For any particular subset of the directional data, averages \bar{D} and \bar{I} are first computed at each site using Fisherian statistics. Key quantities are the data uncertainties σ_D and σ_I . They include contributions from both secular variation (in which we are interested) and within-site errors (which are, or course, undesirable yet unavoidable). The latter are about 3–4 times smaller than the former, when one follows the derivation of JC95 (their Appendix A).

The within-site measurement error σ_j^{wi} for each flow j is derived following e.g. Tarling (1983), using the semi-angle of the 95 per cent confidence cone about the mean direction (that is, a 95 per cent standard error on the mean). JC95 then

estimate the within-site total variances σ_{wi}^2 as the arithmetic averages of the $(\sigma_j^{\text{wi}})^2$ from all flows from the site. The variances associated with secular variation σ_{sv}^2 are calculated at the usual 68 per cent level from the individual directions and their averages. The final total uncertainties in the mean (\bar{D} or \bar{I}), again standard errors on the mean, are simply calculated from

$$\sigma^2 = (\sigma_{\text{wi}}^2 + \sigma_{\text{sv}}^2)/N_l, \quad (4)$$

where N_l is the number of lava flows in the site.

A critical part of the data handling consists of obtaining from the raw data set site averages that will indeed be representative of the mean field, and variances that will embody the influence of secular variation and minimize the importance of palaeomagnetic uncertainties linked to (for instance) proper orientation at the site, recognition of volcano palaeoslopes or tectonic disturbances, proper isolation of the primary remanences in the laboratory, removal of secondary overprints, etc. As noted by JC95, there are often rather large discrepancies between data from nearby sites. This may in part be due to systematic errors, or to the fact that each subset of data consisted of lava flows erupted over too short a period of time to average our secular variation properly. In that case, it is expected that averaging results from nearby sites will lessen the problem and provide more robust and representative data for the inversion. This is discussed further below.

Hulot, Khokhlov & Le Mouél (1997) have shown that, in the ideal case of exact and dense data, directional data would be sufficient to provide a unique model under certain reasonable assumptions.

3 TESTING THE ROBUSTNESS OF THE INVERSIONS

Our aim was to probe as completely as possible the effects of errors and/or uncertainties in the palaeomagnetic data themselves, within the inversion technique, and to evaluate in more detail problems linked with site distribution. We shall now describe the results of a number of inversions pertaining to these three main issues.

3.1 Uncertainties related to the inversion method

As already undertaken by Johnson & Constable, we tested the influence of the starting model in the inversion and found it to be negligible compared with other variations. Hence, the risk of falling into a secondary minimum of the functional does appear to be minimal with their algorithm. We followed the evolution of coefficients resulting from the inversion using the roughness of the model, rms misfit and amplitude of the Lagrange multiplier (JC95, Fig. 6) and, of course, values of each spherical harmonic coefficient as indicators. It was generally found (e.g. Fig. 1) that roughness first increased slowly and rather smoothly, then went through a jagged behaviour with secondary peaks and troughs with rather fast average growth, and then entered a phase where smoother, lesser growth led to saturation. Where the iteration process stops, based on the choice of the tolerance level, with respect to these three states of the roughness curve, varies significantly and may be of some importance. For instance, in JC95's (Fig. 6) example, the iteration stops after passing a first peak in roughness and a very large one in the Lagrange multiplier. It is not clear whether it might not have been safer to stop before these

fluctuations, i.e. stop two iterations earlier, corresponding to a very modest increase of less than 5 per cent in the tolerance level.

The evolution of spherical harmonic coefficients often followed these three phases (Fig. 1). Hence, rather different values could be obtained depending on whether the tolerance was attained in the first or last (smooth) phase. Also, convergence was found to be very sensitive to the amplitude of uncertainties, which is a way to control the final model. A larger uncertainty affecting one or several data will allow a larger discrepancy between model and data. In their Appendix A, JC95 estimate the variance associated with secular variation directly from the data (D_j, I_j) for each flow j in a total series of N_l lava flows as

$$\sigma_{sv}^2(D) = \frac{1}{(N_l - 1)} \sum_{j=1}^{N_l} (D_j - \bar{D})^2, \quad (5)$$

$$\sigma_{sv}^2(I) = \frac{1}{(N_l - 1)} \sum_{j=1}^{N_l} (I_j - \bar{I})^2 \quad (6)$$

(their eqs A7 and A8). This is what they used when next computing total uncertainties with eq. (4). We believe that eqs (5) and (6) actually include all sources of variance, both within-site and secular variation, and therefore provide the best estimates for the total variance. Consequently, we have used as estimates of total uncertainties σ the corrected expressions

$$\sigma_D^2 = \frac{1}{N_l(N_l - 1)} \sum_{j=1}^{N_l} (D_j - \bar{D})^2, \quad (7)$$

$$\sigma_I^2 = \frac{1}{N_l(N_l - 1)} \sum_{j=1}^{N_l} (I_j - \bar{I})^2. \quad (8)$$

As a result, our estimates of uncertainties are approximately 10 per cent less than those of JC95. Although this might appear to be a rather small change, the consequences in the inversions may be quite drastic. As stated by C. Constable

(personal communication, 1997): ‘This is of critical importance since the complexity of models obtained using JC code can be very sensitive to the misfit level selected for the data’. Indeed, the model becomes more constrained and is forced to fit the data with more accuracy at any given level of tolerance. Applying the slightly modified algorithm to a data set as close as possible to that of JC95, we found a number of instances when it became either harder or even impossible to find a convergent solution, or the algorithms converged to a solution that did not fit the data at the given tolerance level. We could either increase the tolerance level or arbitrarily increase the data uncertainties. These are *a priori* undesirable ways of ‘fiddling with the data’. However, the problem is quite severe and significant, and carries some information on the quality (or lack of it) of the data set. Because we had reasons to believe that experimental uncertainties are often underestimated in actual palaeomagnetic studies, and after some numerical experimentation, we decided to increase all uncertainties, as given by eqs (7) and (8), by 10 per cent for the normal data (that is, ironically, returning to values similar to those given by JC95’s original eq. A9), and by 30 per cent for the reversed data (largely because of worse unremoved overprints). We are convinced that experimental knowledge of these total uncertainties is not accurate to even 30 per cent, again underlining that, in many cases, inversions will be worryingly close to not converging, and casting some doubt on the quality of the results when they do happen to converge, given that values of the tolerance level are to a certain degree arbitrary.

In order to ensure that their model had sufficient degrees of freedom, JC95 explored the influence of decreasing the maximum degree of the spherical harmonic expansion. For small values, the inversion often converged to a solution that did not fit the data given the tolerance level. They concluded that maximum degree 10 was adequate to describe the data in all inversions (though they listed model coefficients only up to

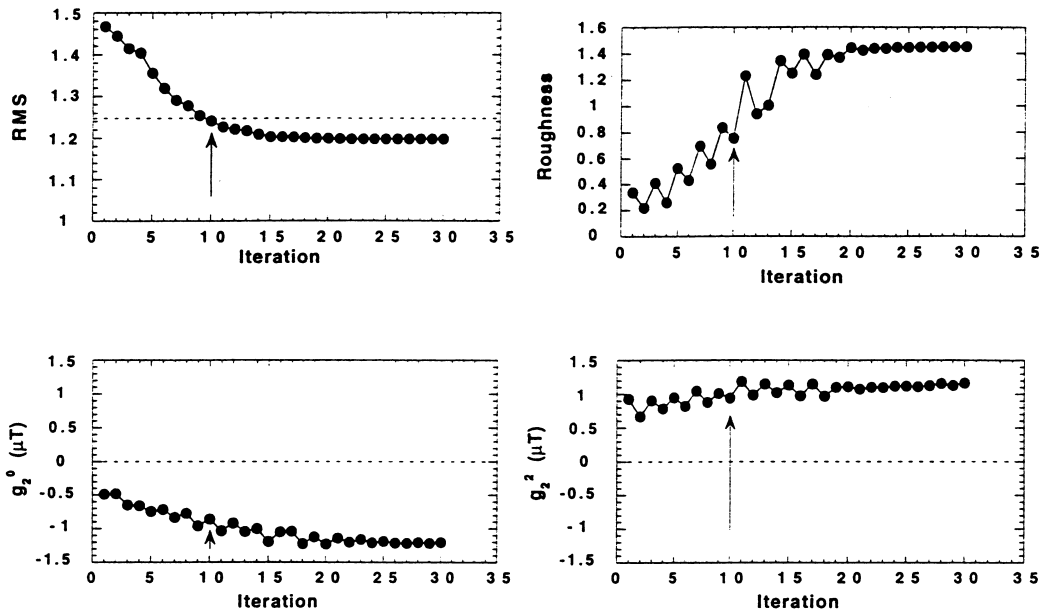


Figure 1. Evolution of some spherical harmonic coefficients (here the quadrupoles g_2^0 and g_2^2) resulting from the inversion of Brunhes data (Q94 data; see Appendix), and evolution of the rms misfit and roughness of the model in a typical inversion. The tolerance level at which inversion is made to stop is indicated by the horizontal dashed line in the roughness curve and the resulting model emphasized with arrows in all parts of the figure.

degree and order 4). We performed a similar analysis (with our modified estimates of uncertainties) and found that, with data set Q94, maximum degree could be lowered to 4, yet was still adequate to estimate the lower-degree harmonics. This is particularly important since it has recently been suggested with growing emphasis that it might be difficult to extract significant models with degree larger than about 3 (Courtillot *et al.* 1992; Kono & Tanaka 1995b; Quidelleur & Courtillot 1996; Hulot & Gallet 1996).

Models from an Occam inversion can be regarded as infinite-dimensional: the number of parameters to be estimated is chosen sufficiently large that addition of further degrees of freedom will not alter the model. C. Constable (personal communication, 1997) notes that truncation at low spherical harmonic degree cannot be regarded as true regularized inversion; indeed, our inverted models, being cut off at low degree, are not the least rough, and increasing spherical harmonic degree may allow the algorithm to find a smoother model fitting the data equally well. C. Constable concludes that our models are in that sense neither truly minimum-norm nor least-squares estimates.

However, a number of observations show that this is probably not a serious limitation. At higher degree, actual values of spherical harmonic coefficients are strongly damped by the regularization of the model, and that damping depends on which regularization criterion is used. For instance, in most of our calculations, the power of degree 5 terms represents

only about 1 per cent of the power of degree 2 terms at the Earth's surface, or 5 per cent at the core–mantle boundary: the regularization constraint is so strong that the robustness, reliability and sensitivity to the data of the higher-order terms are of concern. When JC95 allow the model a large number of free parameters (i.e. 120 for degree 10) and assess that structure only up to degree 4, they fail to discuss those terms which have been most affected by the chosen regularization. Furthermore, using real data sets, we found that increasing maximum degree from 4 up to 10 did not alter the characteristic features of the field at the CMB: an example is shown in Fig. 2. We see that the behaviour of field contours does not change much, particularly where there are denser data. High-latitude lobes, such as found by Gubbins & Kelly (1993), are not seen, even with maximum degree 10. The major difference is a shorter-wavelength anomaly in the Pacific, constrained by the Hawaiian data. As a result, we selected a maximum harmonic degree of 4 for both field inversion and graphic display.

3.2 Uncertainties related to the JC96 data set

We have next investigated the effect of the data and of the data set structure itself. In order to allow our new results to be compared with those previously published by Johnson & Constable, we first applied their inversion scheme to the data set that they had assembled (JC96). As done by previous

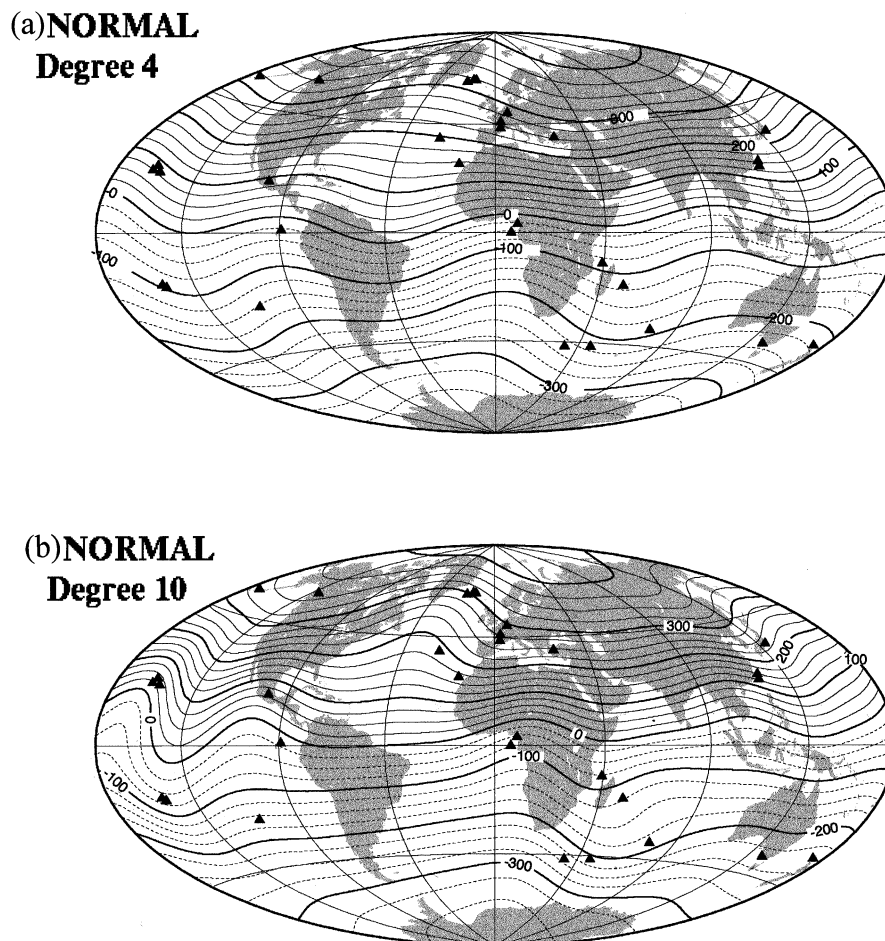


Figure 2. Maps of the radial component B_r at the core–mantle boundary for the Q94-me normal data set; see Appendix. Contour interval is $25 \mu\text{T}$. Triangles show sites where data are available. The maximum degree reached in the inversion is 4 (a) and 10 (b).

authors, three main subsets of the data were generated: all Brunhes epoch data (index B), all normal data for the past 5 Myr (index N), and all reversed data (index R). JC95 found that a number of data had an unexpectedly large and most likely undesirable effect on the inversions. Therefore, they eliminated those subgroups of data: these were four of the B data (Hawaii, Pagan Island, Crozet and Japan), five of the N data (Caribbean, Fernando de Noronha, Libya, Norfolk Island and Madagascar), and three of the R data (Libya, Sicily and Norfolk Island). On the other hand, we used our own estimates of uncertainties as discussed above. Finally, we decreased the maximum degree requested in the inversion and selected as an optimal value the lowest at which the tolerance level was first achieved. This led us to a maximum degree of 3 for the B and R data, and 4 for the N data. In order to allow more homogeneous comparison of our models one to the other, and with those published by Johnson & Constable, and also for the reasons outlined in the previous subsection, we use a maximum degree of 4 for all data subsets.

For each modified data subset (B, N and R), new perturbed data sets were produced by adding to the data set values of \bar{D} and \bar{I} random perturbations compatible with uncertainties σ_D and σ_I , assuming a Gaussian distribution. Results are presented in Fig. 3 and listed in Table 1(b). The values originally found by JC95 using a jack-knife approach are listed for comparison in Table 1(a). Individual results from 15 experiments each are shown on the left side of Fig. 3, in order to visualize better the spread of the results, while averages for all experiments are shown on the right side, together with their standard deviations (*not* their standard errors).

As noted by Johnson & Constable, and found by many researchers since Wilson (1970, 1971), the axial quadrupole g_2^0 is generally seen to be the dominant term in the inversion (see Section 4). Other apparently important terms (i.e. significantly different from zero, given formal uncertainties and/or spread of inverted results) are:

- (1) *for the B data*, the equatorial dipole g_1^1 (of the order of 60 per cent of g_2^0), the h_2^1 and g_2^2 quadrupoles (50 per cent of g_2^0) and possibly the g_3^0 axial octupole (30 per cent of g_2^0);
- (2) *for the N data*, h_3^1 (70 per cent of g_2^0) and to a lesser extent g_4^1 , h_4^1 and h_4^2 (around 35 per cent of g_2^0) and h_2^2 (30 per cent of g_2^0);
- (3) *for the R data*, g_1^1 , g_2^1 , h_2^1 , g_2^2 (between 35 and 50 per cent of g_2^0) and h_1^1 , h_2^1 , g_3^0 , g_3^3 and h_3^3 (15–20 per cent of g_2^0).

All other coefficients have either much smaller amplitude or a range that includes zero. It may be worth recalling that, although individual harmonic coefficients have no physical significance in themselves, they indicate the contribution of each individual spherical harmonic base function. Also, they allow a comparison of the importance of zonal versus non-zonal, dipole versus non-dipole terms, or comparison of two different inversions. Only the total combination, however, gives a global view of the model and the quality of its fit to the data.

Referring to Table 1(a), we can next compare the results obtained by JC95 with those that we derive. In this discussion, as in much of what follows, we use an arbitrary threshold of 300 nT, to be justified later, below which inverted model coefficients are not considered by us to be significantly different

from zero (hence, 300 nT or smaller amplitude will be considered as ‘negligible’). In that sense, both sets of inversions reveal five large coefficients for the Brunhes data, in addition of course to the axial dipole. Three are the same in both studies (g_1^1 , g_2^0 and g_2^2), although all tend to be somewhat larger in our calculation, from 10 to 30 per cent, and even 50 per cent for the equatorial dipole. This may in part be due to inversion being stopped at degree 4. On the other hand, the fourth largest harmonic is shifted from g_2^1 in JC95 to h_2^1 in our calculation. All other terms are identically ‘small’ or ‘negligible’ in both studies. We can consider this both as rather good agreement and as a first indication of the robustness (or lack of it) of model coefficients.

For the normal data, there are seven ‘large’ terms in both studies. Good agreement is found for g_2^0 , g_2^2 (and h_2^2), g_3^0 , h_3^1 , g_3^3 , h_3^3 , g_4^1 , h_4^1 and h_4^2 . In some cases, a coefficient is below our threshold of 300 nT according to one inversion, above according to the other. Notable differences are a much larger equatorial dipole in JC95 (almost three times), a large h_2^1 , which we do not find, a rather large h_3^2 in our case, and a large g_4^3 in JC95. The JC95 N model has in general more energy in more terms.

The R data provide in both cases much larger amplitudes, which are more likely to reflect problems with data quality and distribution than geomagnetic features. We find some 10 rather large terms. Ratios of amplitudes of those terms to those found by JC95 range from 500 to 1600 nT (1300 nT for the axial quadrupole). Except for g_1^1 , g_2^0 , g_2^2 and g_3^1 , which are quite similar (or lower in JC95), all other terms seem to be 2–3 times smaller in our case. JC95 find rather large degree 4 terms, which we do not find.

3.3 Uncertainties related to the data—*influence of a single site*

After having checked the effects of using basically the same algorithm on the same data set, though with some modifications, the next step was to analyse the effect of the contents of the data set itself. We therefore applied exactly the same algorithm to subsets of the Q94 data set proposed by Quidelleur *et al.* (1994). Criteria for building that set were given in that paper, and were rather similar to those applied by Johnson & Constable (JC96) in their updated version of the Lee data set. There were some differences, however, which are summarized in the Appendix. This Appendix also provides abbreviated codes for various versions of the data sets used throughout this paper. The tests that follow have been performed on an updated, modified data set, Q94-m. We will first illustrate problems resulting from individual data with previously unexplained or unspotted major effects, then resume comparison with the JC95 results.

A striking effect is easily identified in a display of results from inverting the R data of the Q94-m data set, when a jack-knife approach is applied to the data (Fig. 4). More precisely, the data set contains directions from 22 distinct geographical sites. The jack-knife technique consists of performing the inversion 22 times, removing all data from one and only one given site at each time. Inspection of Fig. 4 shows that data from a single site clearly perturb the inversion, this site being located in Ethiopia (Schult 1974). Unreasonably large values of g_1^1 , h_1^1 , g_3^0 and h_3^1 are obtained when the Ethiopian data are included, whereas all coefficients become smaller or even

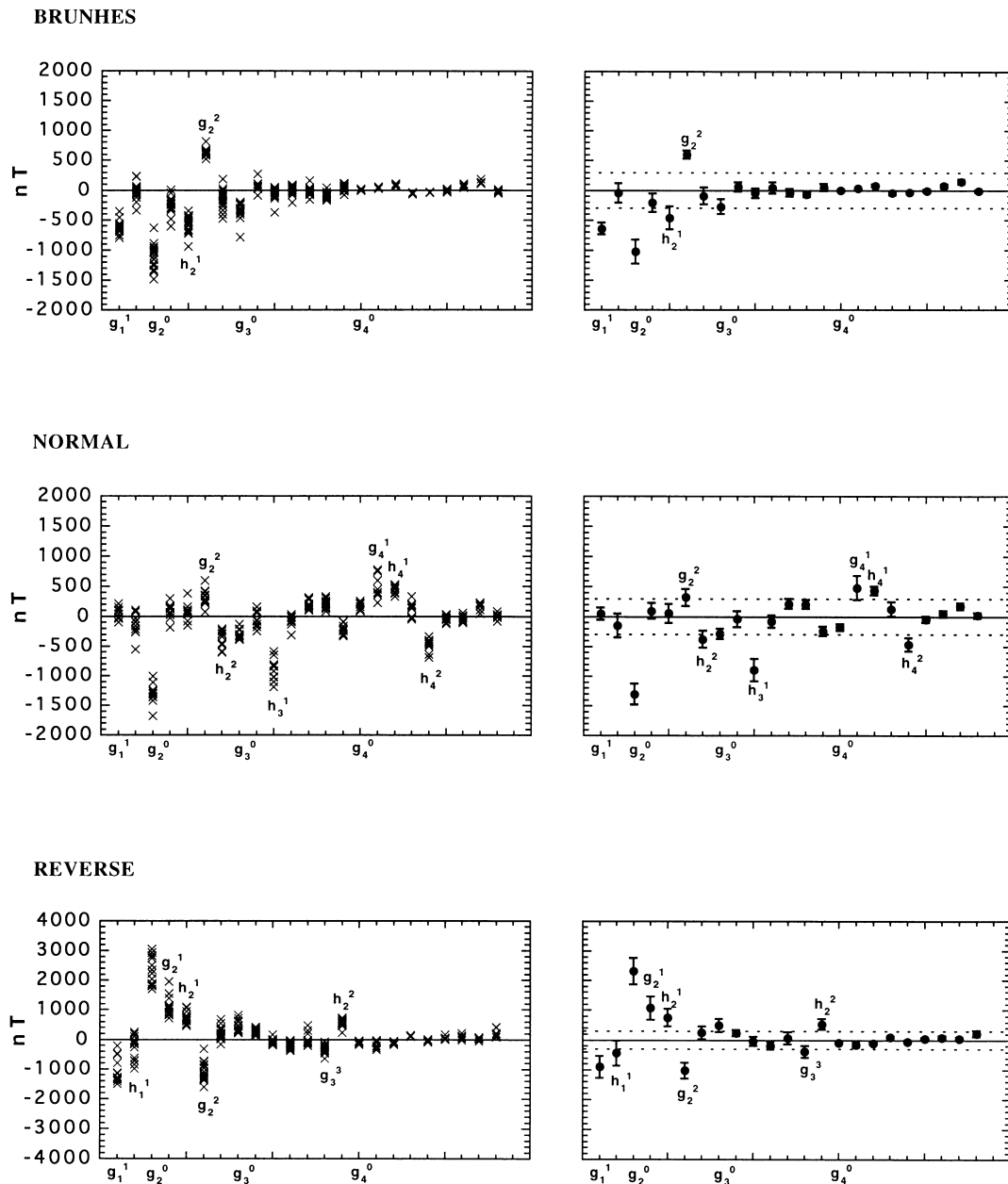


Figure 3. Inverted spherical harmonic model coefficients up to degree and order 4 for the JC96-2 data (Johnson & Constable 1996; see Appendix), using the JC95 algorithm (Johnson & Constable 1995) as slightly modified and discussed in this paper (see text). Left side displays results from 10 inversions each, successively for the Brunhes, normal and reverse data subsets. Each inversion is based on the JC96 data set, adding to the published data random Gaussian noise compatible with revised values of uncertainties (see text). Right side displays corresponding mean values and standard deviations, emphasizing with dashed lines at ± 300 nT the range about zero in which it is argued that the model coefficients may not be significant. The maximum degree reached in the inversion is 4.

negligible when they are not. The amplitude of the axial quadrupole is also reduced by a factor in excess of 2. The overall behaviour is particularly conspicuous in a graph of model roughness: this is 3–4 times less when the Ethiopian data are excluded. The Schult (1974) data happen to come from a particularly complex and tectonically active area, the Afar depression and triple junction, in which our group has gathered extensive tectonic, palaeomagnetic and geochronologic data over the past 15 years (Courtillet *et al.* 1984; Manighetti 1993; Manighetti *et al.* 1997; Kidane *et al.*, in preparation). We now know that much of the Afar is floored by a basaltic series,

with ages concentrated around 2 Myr, which has been dissected into rotating blocks by continental rifting and rift propagation (Courtillet 1980; Tapponnier *et al.* 1990; Manighetti *et al.* 1997). This has resulted in heterogeneous rotations of blocks about vertical axes by up to 15° . As a result of this tectonic activity, these data cannot be included in a data set for the purpose of geomagnetic analysis. New samples, collected south of the depression in the apparently unrotated termination of the East African Rift, should soon provide a more acceptable datum (Kidane *et al.*, in preparation). The Ethiopian data are the only ones to provoke such extreme effects on the inversion,

Table 1. Inverted field models for different sets of the Brunhes (B), normal (N) and reversed (R) data using the method of Johnson & Constable (1995) as modified and discussed in this paper. (a) Data from Johnson & Constable (1996, JC96-2), evaluation of standard errors S_g and S_h on g_l^m and h_l^m using a jack-knife approach. Maximum degree of inverted models set at 10. (b) Data from Johnson & Constable (1996, JC96-2), with data uncertainties as modified in this paper (eqs 7 and 8) and standard deviations (σ_g and σ_h) instead of standard errors. Maximum degree of inverted models set at 4. (c) Data from Quidelleur *et al.* (1994, Q94-me). Otherwise as in (b).

(a) JC96-2 data					(b) JC96-2 data, modified					(c) Q94-me data				
Brunhes Field Model														
<i>l m</i>	g_l^m	h_l^m	s_g	s_h	<i>l m</i>	g_l^m	h_l^m	σ_g	σ_h	<i>l m</i>	g_l^m	h_l^m	σ_g	σ_h
1 0	-30 000	0	0	0	1 0	-30 000	0	0	0	1 0	-30 000	0	0	0
1 1	-436.7	-90.2	45.8	33.1	1 1	-645	-48	98	161	1 1	-564	374	177	140
2 0	-987.9	0	22.5	0	2 0	-1025	0	195	0	2 0	-808	0	201	0
2 1	-484.8	-263	17.7	10.3	2 1	-209	-464	153	191	2 1	104	-313	88	104
2 2	564.8	-135.9	17	10.4	2 2	600	-95	70	139	2 2	554	-237	67	107
3 0	-310.6	0	10.3	0	3 0	-274	0	122	0	3 0	-37	0	40	0
3 1	-27.5	-99.3	5.5	6.6	3 1	58	-49	73	83	3 1	-8	-114	30	67
3 2	-43.9	0.7	8.5	4.3	3 2	43	-45	95	63	3 2	144	-101	47	34
3 3	-73.8	-223.4	6.3	12.7	3 3	-75	47	41	59	3 3	-198	75	78	106
4 0	36.4	0	2.7	0	4 0	-3	0	12	0	4 0	19	0	27	0
4 1	4.4	80	2.1	3.6	4 1	35	76	13	23	4 1	-33	17	30	13
4 2	27.5	-91.1	3.5	4.4	4 2	-50	-35	29	9	4 2	16	-48	18	33
4 3	-0.2	-5.1	2.3	2.1	4 3	-10	72	22	30	4 3	-20	19	22	12
4 4	132.5	104.6	6.5	5.3	4 4	140	-15	42	22	4 4	104	-8	49	28
Normal Field Model														
<i>l m</i>	g_l^m	h_l^m	s_g	s_h	<i>l m</i>	g_l^m	h_l^m	σ_g	σ_h	<i>l m</i>	g_l^m	h_l^m	σ_g	σ_h
1 0	-30 000	0	0	0	1 0	-30 000	0	0	0	1 0	-30 000	0	0	0
1 1	209	395	18.4	20.9	1 1	47.6	-148	95	188	1 1	44	235	177	220
2 0	-1334.4	0	14.7	0	2 0	-1305	0	178	0	2 0	-1093	0	186	0
2 1	37	-282.8	15.5	19	2 1	92	54	133	157	2 1	89	-391	201	246
2 2	264.4	-212.9	10.8	9	2 2	321	-379	142	143	2 2	336	-222	130	97
3 0	-467.3	0	11	0	3 0	-287	0	86	0	3 0	-275	0	150	0
3 1	-45.6	-822.1	11.3	13.5	3 1	-39.5	-897	131	190	3 1	250	-440	222	187
3 2	-56	31.3	8.1	9.4	3 2	81	214	93	80	3 2	-155	69	124	82
3 3	388.7	-292.1	9.2	5.3	3 3	207	-242	76	74	3 3	90	12	114	133
4 0	139.2	0	6.6	0	4 0	-178	0	54	0	4 0	140	0	94	0
4 1	313	265.2	7.2	6.6	4 1	482	430	177	72	4 1	85	23	88	76
4 2	231.2	-466.2	9.2	7.2	4 2	129	-470	120	112	4 2	75	-180	131	49
4 3	-290.7	-33.7	7.5	5.3	4 3	-43	43	51	54	4 3	-160	-72	92	81
4 4	104.9	-77.1	6.5	5.3	4 4	175	19	57	46	4 4	264	-2	129	86
Reverse Field Model														
<i>l m</i>	g_l^m	h_l^m	s_g	s_h	<i>l m</i>	g_l^m	h_l^m	σ_g	σ_h	<i>l m</i>	g_l^m	h_l^m	σ_g	σ_h
1 0	30 000	0	0	0	1 0	30 000	0	0	0	1 0	30 000	0	0	0
1 1	-911.6	-1221	54.2	48.9	1 1	-905	-445	363	420	1 1	-111	-460	219	330
2 0	1980	0	48	0	2 0	-2320	0	448	0	2 0	1680	0	556	0
2 1	1531.4	1234.4	35.2	47.4	2 1	1067	750	393	286	2 1	190	613	308	169
2 2	-679.9	704.3	36.9	29.6	2 2	-1030	248	270	211	2 2	-126	316	210	193
3 0	1097.3	0	39.8	0	3 0	491	0	217	0	3 0	520	0	148	0
3 1	0.3	-651.4	23.2	33.9	3 1	231	-40	97	159	3 1	-226	165	126	113
3 2	119.1	86.8	36.3	18.2	3 2	-187	67	130	209	3 2	-201	205	109	121
3 3	-554.3	474	14.6	31.8	3 3	-394	531	195	177	3 3	-412	371	181	88
4 0	-85.8	0	7.3	0	4 0	-87	0	38	0	4 0	51	0	19	0
4 1	-485.3	-212.2	17.1	10.1	4 1	-160	-110	93	42	4 1	-73	-11	21	25
4 2	181.1	-8.1	9.6	11.7	4 2	97	-53	35	40	4 2	-57	56	28	33
4 3	141.9	78.9	13.3	13.4	4 3	38	87	48	67	4 3	-88	153	51	48
4 4	308.9	331.3	18.1	5.3	4 4	44	217	49	108	4 4	-121	-112	57	39

as illustrated by Fig. 4. However, many data come from active areas, and smaller yet significant tectonic effects might still remain. Indeed, few of these palaeomagnetic sites have been constrained by detailed tectonic analysis.

3.4 Uncertainties in the data—the Q94 data set

Following the above observations, the inversion was resumed with the Q94-m data set, excluding the Ethiopian site

(data set Q94-me following the Appendix). This was done in the same way as JC96, and the results are shown in Fig. 5 and listed in Table 1(c). Although the two data sets yield broadly similar results, particularly as regards the most important coefficients, it is interesting to point out a number of significant differences. In the discussion of ‘significant’ or ‘small’ coefficients, we still retain the 300 nT threshold as a useful separator.

Given that threshold, we find for the B data that g_3^0 has much reduced amplitude and may not be significant any more.

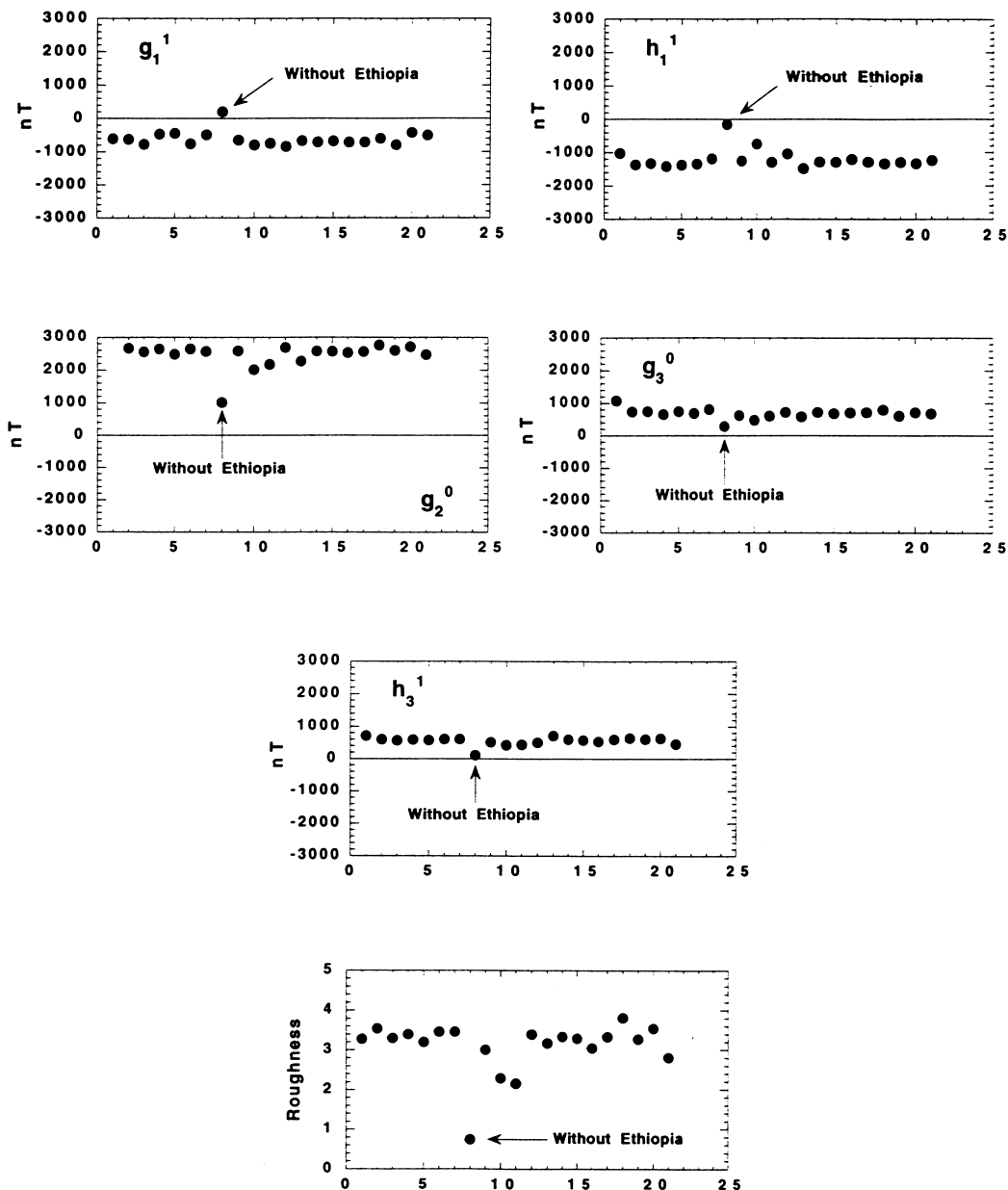


Figure 4. Selected inverted spherical harmonic coefficients (g_1^1 , h_1^1 , g_2^0 , g_3^0 and h_3^1) using the modified Q94-m data set (see text and Appendix). Inversion is made by removing one site at a time (jack-knife approach). There are 21 such inversions, number 8 corresponding to the case when the data from Ethiopia (Schult 1974) are removed. At the bottom is shown the evolution of model roughness during these tests.

On the other hand, h_1^1 , which was not significant in the JC96 data, becomes as significant as h_2^1 . Although still within the 300 nT band about zero, g_3^0 increases in amplitude. For the N data, the only term other than the axial quadrupole that was quite large in the JC96 data, g_3^1 , has become reduced to the edge of significance. It is particularly interesting that, in the N data, all other terms now have uncertainties that include or come very close to zero. In the R data, three previously significant terms, g_1^1 , g_2^1 and g_2^2 , have now become insignificant. On the other hand, g_3^3 has become larger and g_3^1 has changed sign (though on the edge of significance).

Altogether, and limiting our analysis to degree and order 3 for the three data sets (B, N, R), six terms that were very significant (i.e. larger than 800 nT) in the JC96 data have become less significant (if even significant), two others have

become significant though not very large, and a couple have changed sign. This, of course, casts serious doubts on the robustness and actual geomagnetic meaning of these terms.

3.5 Sources of data uncertainties

A number of sources of uncertainty exist in the collection of palaeomagnetic samples and the production of remanence directions in the laboratory. These include orientation errors, undetected or uncorrected palaeoslope values and tectonic rotations, and undetected and/or unremoved magnetic overprints. Most palaeomagnetic data in the sets come from active volcanoes associated with hotspots. Although these often produce fluid basaltic lavas, significant palaeoslopes may occur and it is not always clear in the original paper whether these

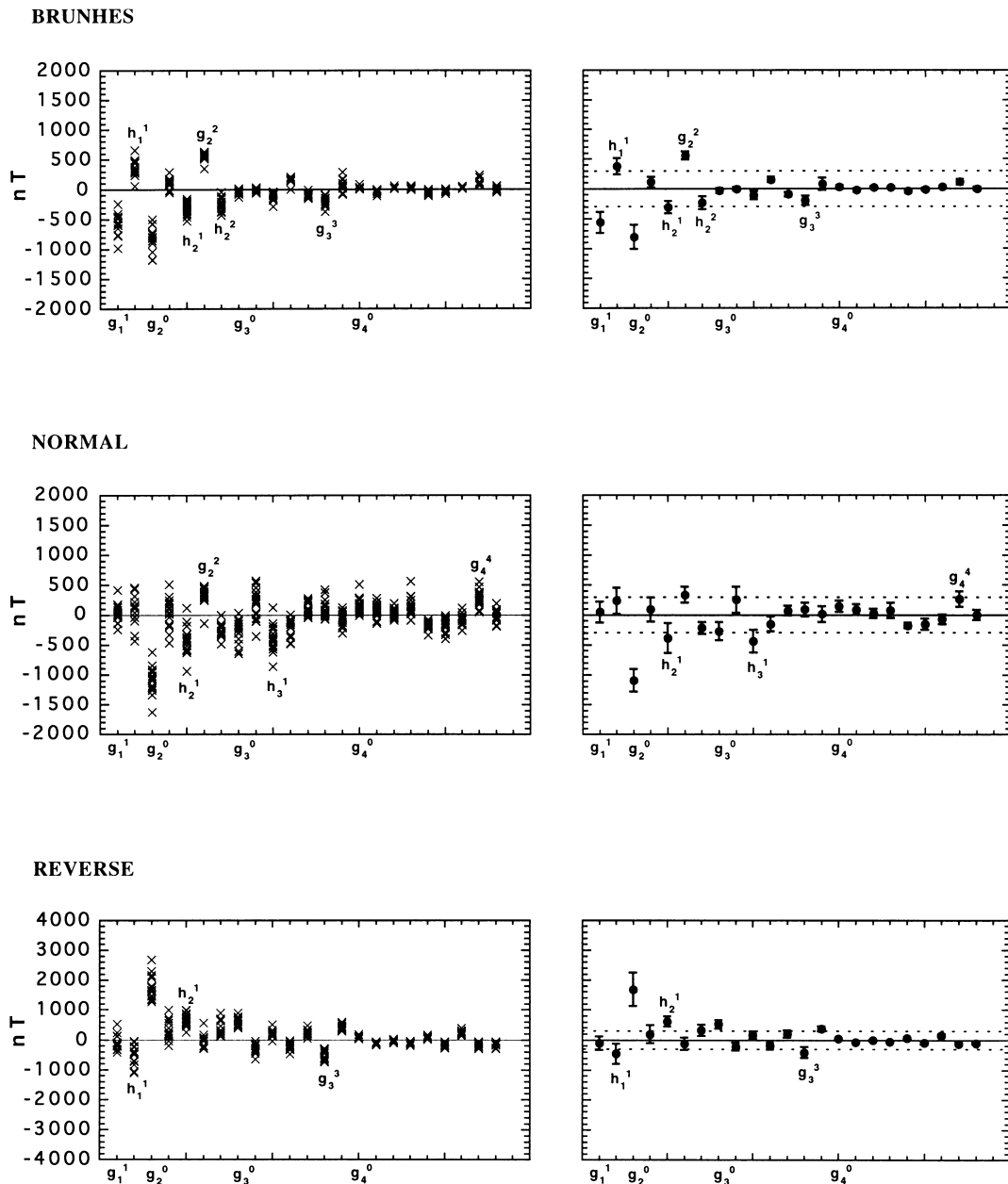


Figure 5. Same as Fig. 3 for the modified Q94-me data set (see text and Appendix), with the data from Ethiopia removed (see Fig. 4).

have been measured and taken into account. The case for tectonic rotation can be particularly worrying; for instance, it is reasonably well studied and understood in the Afar case, as seen in the previous section, but smaller tectonic rotations in the range normally attributed to secular variation may well have gone undetected.

A recent example is given by Tanaka *et al.* (1996), who studied Brunhes- and Matuyama-age deposits from the central Taupo Volcanic Zone in New Zealand. These authors find what they believe to be otherwise correlative units yielding divergent palaeomagnetic directions, which could be due either to actual (fast, high-amplitude) palaeosecular variation (PSV), or to extensional tectonics in this very active area. Strangely enough, the younger normal polarity sites appear to have undergone a clockwise rotation, whereas the older normal polarity sites give a mean that is indistinguishable from the direction

expected from a geocentric axial dipole. Fig. 1 from Tanaka *et al.* (1996) shows that most normal sites are located with the Taupo Volcanic Zone, whereas the reversed ones tend to be located outside. We might therefore suggest that the heavily faulted Taupo Volcanic Zone has undergone more tectonic deformation, resulting in rotations about vertical axes, than its surroundings. Hence, the reversed New Zealand data might be acceptable for PSV analysis, whereas the normal ones should probably be rejected. Further study of this is in progress (Tanaka *et al.* 1996).

Another source of uncertainty, which we have analysed in a little more detail, stems from unremoved viscous or secondary magnetic overprints. An increasing number of case studies indicate that such overprints may bias the directions of what were otherwise thought to be clean primary remanence directions. This may be easy to detect when the directions of

the primary and secondary components are very different (e.g. Vandamme *et al.* 1991), but becomes far more difficult when they are similar. As an exercise, we have generated artificial sets of B, N and R data by assuming that an overprint in the direction of the present Earth's field (actually the 1980 IGRF) was still present in the Q94-me data set. We have removed small vectors in the direction of the 1980 IGRF, assuming their amplitude to be 5 per cent of that of the natural remanent magnetization (NRM). Rather than comparing each individual coefficient, we evaluate the power in each one of the first three degrees, using the Lowes (1974) formula:

$$R_l = (l+1) \sum_{m=0}^l [(g_l^m)^2 + (h_l^m)^2]. \quad (9)$$

The axial dipole is not included in the case $l=1$, where only power related to the equatorial dipole is evaluated. Results are shown in Fig. 6. Though they were already the smallest in amplitude, the equatorial dipole terms were least affected, being orthogonal to the dominant g_1^0 , which is removed in the modelled overprint. The $l=2$ terms were significantly decreased in the case of the B and R data. For the $l=3$ terms, the R data led to the largest power reduction, whereas the N data led to an increase, B being hardly affected. Altogether, removing a normal overprint led to a simpler field model with less energy in the higher harmonics. This was clear for instance for the significant decrease of h_3^1 , leading one to suggest that this might typically be an artefact of unremoved overprints (given the very oversimplified geometry of our overprint model).

A similar exercise was performed by McElhinny, McFadden & Merrill (1996). They assumed a fully zonal mean-field model and inverted the data in the form of the latitude distribution of the inclination anomalies (departures from inclinations predicted for a geocentric axial dipole). They generated a field model with only g_1^0 and g_2^0 contributions at the actual sites of the data set, injected a 5 per cent normal overprint and inverted the resulting 'observations'. A g_3^0 with an amplitude comparable with g_2^0 was found, which could only be an artefact.

Although such numerical experiments can only provide order-of-magnitude estimates, they cast very strong additional doubts on the geomagnetic significance of terms other than g_1^0 and g_2^0 . Returning to Fig. 6, we notice that the equatorial dipole, which is likely to be the easiest term to extract in the inversion, has the smallest amplitude. With a now generally accepted amplitude between 1000 and 2000 nT, g_2^0 should contribute about $6 \times 10^6 \text{ nT}^2$ to the power of quadrupole terms. This is the amplitude of the B and N power estimates. The largest power, almost double the expected value, is found for the R data, i.e. the least well determined, the ones with the smallest data set and worst geographical distribution, the most susceptible to the effect of overprints. Interestingly, the power in g_2^0 decreases when one attempts to model the effect of overprinting. As far as the octupolar terms are concerned, the B and N data happen to yield a power similar to that in the equatorial dipole, i.e. quite low. The R data on the other hand have as much power as the quadrupole, but they are the most affected by overprinting. Hence a large part of the power seen in the inverted R models may result from a number of sources irrelevant to geomagnetic field modelling.

3.6 Uncertainties related to site distribution

Many authors have mentioned the fact that the number of geographically separate sites was unfortunately small and their distribution very heterogeneous. We are actually viewing the palaeofield through a particularly distorted spatial sampling scheme (a sort of 'antenna') and this may naturally result in various forms of potentially serious aliasing. In Fig. 7, we have mapped the average distance between each site and its neighbours (actually the arithmetic mean of the angular distance of one site to all the other ones). For the B data, more than half of the Earth (the Pacific hemisphere) shows distances in excess of 60° . For the R data, this applies to all of the Earth, except locally near Europe, North Africa and the North-East Atlantic. This would in itself (*a priori*) raise doubts as to the possibility of extracting valid global estimates of harmonics with degree

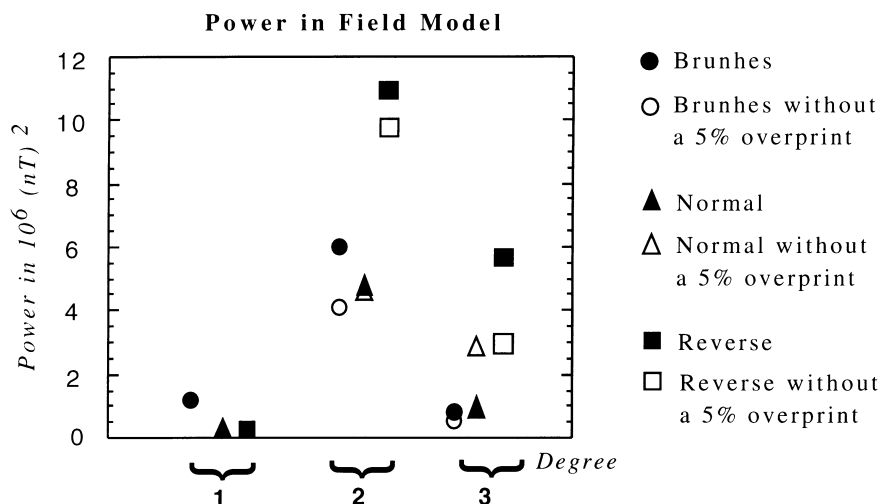


Figure 6. Power spectrum of each inverted field model for the first three degrees using the Lowes (1974) formula. The axial dipole g_1^0 has been excluded when calculating power in the $n=1$ terms. Full symbols are for data from the Q94-me data set (see Appendix), for the Brunhes, normal and reversed subsets. Open symbols are for the same data after removal of a present-day normal overprint (IGRF 1980) with amplitude equal to 5 per cent of the NRM.

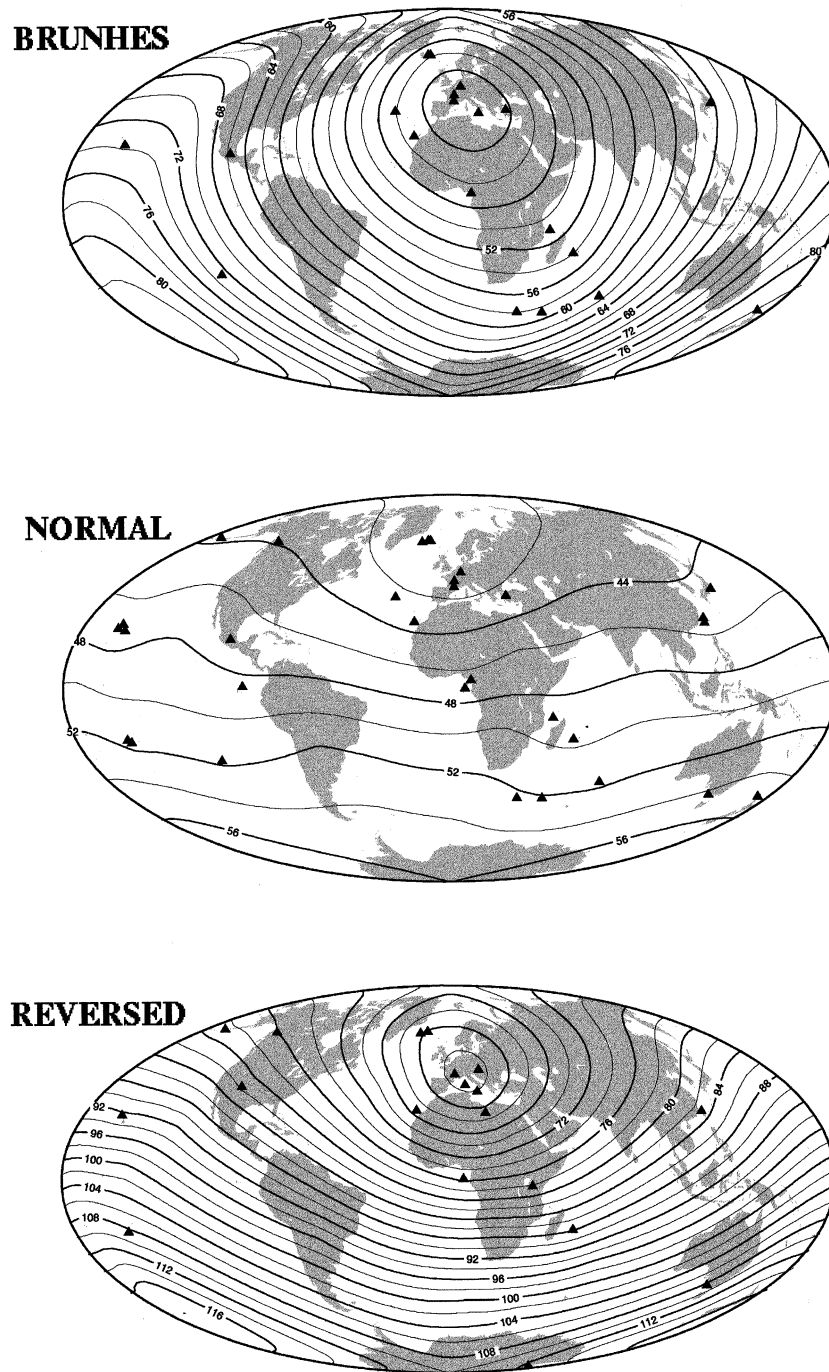


Figure 7. Average angular distance in degrees between any site and all of its neighbours for the Brunhes (B), normal (N) and reversed (R) subsets of data from Q94-me (see Appendix).

equal to or in excess of 3. The areas with denser sites may of course lead to aliasing in less well constrained zones (i.e. the majority of the Earth's surface in all cases but the N data, for which average spacing is everywhere between 40° and 55°).

The influence of site distribution can be tested in various ways. A simple way is to generate artificial data for simple field models, invert them and compare the results to the input. In this way, we have generated seven field models, each of which involves a constant axial dipole ($g_1^0 = 30 \mu\text{T}$) and a single other term of $1 \mu\text{T}$ amplitude, going up to degree and order 2. We have generated directions from these models at

the exact site locations where data are available for each subset, and inverted them up to degree and order 3. This is a simple way of investigating the cross-correlation of model parameters in the inversion. The maximum values of non-diagonal terms are of the order of $0.1 \mu\text{T}$ and can reach $0.2 \mu\text{T}$. For example, a $1 \mu\text{T}$ g_2^0 in the B site distribution generates through aliasing equatorial dipole components $g_1^1 = 92 \text{ nT}$ and $h_1^1 = 123 \text{ nT}$, and also $h_2^2 = 76 \text{ nT}$ and $h_3^2 = 74 \text{ nT}$. A $1 \mu\text{T}$ g_2^1 (in the N site distribution) generates $g_1^1 = 178 \text{ nT}$, $g_2^0 = 85 \text{ nT}$, $g_3^1 = 72 \text{ nT}$, ... In addition, note that the diagonal term that is recovered (i.e. the $1 \mu\text{T}$ harmonic used in generating the

synthetic data) is itself recovered with an error ranging from -200 to -400 nT (always with the same sign, that is an underestimate by up to 40 per cent).

4 DISCUSSION AND CONCLUSIONS

Courtillot *et al.* (1992) argued that, given data quality and remaining differences between models, it seemed difficult to demonstrate that the long-term (1 Myr) average geomagnetic field contained any persistent feature beyond the g_1^0 axial dipole. The rest appeared to behave like random noise, the present-day non-axial-dipole field being a typical sample of this random noise. However, further work by many authors has confirmed the presence of a small persistent axial quadrupole g_2^0 , first discovered by Wilson (1971). However, all other terms remain a matter of controversy.

We can use the various results from the previous sections to place further constraints on those. The exercise leading to the calculation of influence matrices has shown that, all other features being constant, a $1 \mu\text{T}$ quadrupole would alias into other components, most notably the equatorial dipole with amplitudes of the order of 0.1 to $0.2 \mu\text{T}$. This is largely due to the very inhomogeneous distribution of the approximately 20 sites where data are available. Comparing results from inversions performed by various authors on various data sets (e.g. Gubbins & Kelly 1993; JC95; this paper), and comparing within the same study inversion of B, N and R type data, give a further idea of the threshold under which individual terms cannot be considered as significantly different from zero. As a matter of convenience, we propose that this threshold is of the order of $\pm 0.3 \mu\text{T}$. This is taken to represent the rough limit of resolution beneath which it is difficult to decide whether a coefficient has real significance or is just an artefact.

Given that threshold, very few terms stand out clearly in a robust fashion. The g_1^1 equatorial dipole for instance is reduced when one goes from the Johnson & Constable data set (Fig. 3) to ours (Fig. 5), and is completely absent in the N and R data. It is therefore reasonable to assume that the geomagnetic equatorial dipole averages to zero over these timescales (consistent with all ideas in dynamo models regarding the role of Coriolis force), and that it does not average out in our B data because of, for instance, poor site distribution or remaining recent overprints. Also, a g_2^2 term of about $0.6 \mu\text{T}$ appears in the B data (for both the Q94-me and JC96-2 data sets), but is at or below the $0.3 \mu\text{T}$ threshold in the N or R data. There is also a h_3^1 term of $-0.6 \mu\text{T}$ in the N data, but in neither the B nor the R data. It is this h_3^1 term which suffers the largest reduction when going from the JC96 to the Q94 data set. As noted above, three terms in the R model that appeared in the JC96 results (g_1^1 , g_2^1 and g_2^2) are not significant any more in our results. Finally, if we check which coefficients (except g_2^0) are both significant and common to the two data sets, we find only g_2^2 and g_1^1 for the Bunhes data, and h_2^1 and g_3^0 for the reverse data. These terms should therefore be the prime candidates for further testing of robustness and significance. Given the tests of McElhinny *et al.* (1996), not much confidence for instance can be placed on the reality of any g_3^0 . If we add the condition that coefficients should belong to all three data subsets, only g_2^0 remains.

Thus, these inversions strongly suggest that only g_1^0 and g_2^0 may be sufficiently robust to the various changes in method, data set, etc. Therefore, a model where only these two axial terms are non-zero and all other coefficients do average out to zero appears to be consistent with the data and the confidence we can place in them. This is essentially the structure of the CP88 (Constable & Parker 1988) giant Gaussian process, recently further explored by Quidelleur & Courtillot (1996). We will return later to its variance structure.

As noted before, McElhinny *et al.* (1996) have recently explored a complete palaeomagnetic database. They argue, based on declination anomalies, for the lack of significance of any non-zonal variations, but fail to explore this in a systematic way. However, our own results provide a firmer basis for this proposal. Our study leads us to confirm that the g_2^0/g_1^0 ratio is of the order of 4 per cent, ranging from 3.5 to 5.5 per cent. Original estimates by Merrill & McElhinny (1997) were in the range of 5 to 8 per cent, estimates based on sedimentary data from 3 to 5 per cent (Schneider & Kent 1988). The recent analysis of inclination anomalies by McElhinny *et al.* (1996) leads to 3 to 4 per cent. These values are in rough agreement, with the more recent ones tending to be on the lower side of earlier ranges. Taking arbitrarily a mean value for the axial dipole of the order of $30 \mu\text{T}$ would lead to an axial quadrupole between 1 and $1.5 \mu\text{T}$. The above analysis fails to provide convincing support, again within current uncertainties in the data, for other persistent features (such as an axial octupole g_3^0), or for north versus south hemispherical asymmetry or for normal versus reversed polarity asymmetry. A contentious issue is that of the persistence of higher-latitude flux concentrations (Gubbins & Kelly 1993). We do not observe such features, though our maximum degree of 4 may not be sufficient for their identification. We note, however, that, as data quality and methods progress, these become less and less apparent (see note added in proof at the end of the paper).

We can use our preferred model to generate maps of the mean field, which can be compared to the original data (D, I), or continued downwards at the CMB. Examples of the latter for the radial (vertical) component B_r are shown in Fig. 8. Not surprisingly, our maps tend to be smoother than (though quite similar to) those of JC95 actually generated after removal of 'anomalous' sites (their Figs 13–15, models LB2, LN2 and LR2). This is particularly true for the reversed data. Oscillations or features tend to appear in areas with the least constraints, i.e. the Southern Hemisphere and the Pacific Ocean. For the B data, the magnetic equators we find fluctuate about the geographic equator, but they are not in phase between the JC96 (LB2) and our model. For the N data, JC96 (LN2) have complex features that we do not see in the Pacific between Hawaii and Tahiti. Recall, however, that our inversion is stopped at $n = 4$, whereas JC95 calculate models up to degree and order 10.

Declination and inclination anomalies (with respect to the pure axial dipole model) are of potential interest in a number of palaeomagnetic applications. Again, it is interesting that inclination anomalies (Fig. 9) do not exceed about 3° near where data are actually constraining the model. For the Brunhes data, the anomaly reaches -4° in New Zealand, and the strong (-9°) anomaly in the western-central Pacific is entirely unconstrained by local data; 16 out of 20 sites have ΔI less than 2° . Anomalies tend to be smaller (due to more

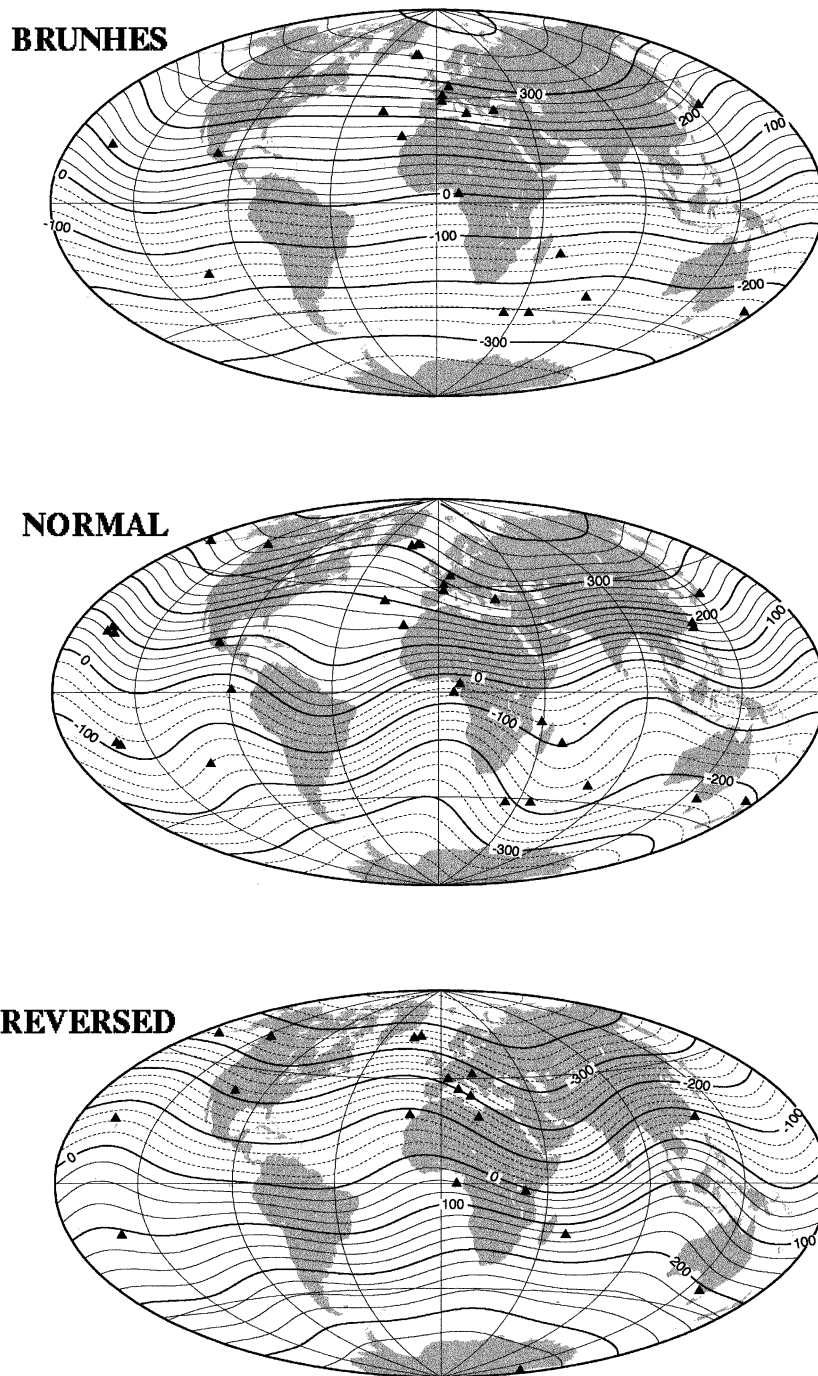


Figure 8. Average field model resulting from the inversion of the Q94-me Brunhes (B), normal (N) and reversed (R) data up to degree 4 (see Appendix). This is shown as a map of the radial component B_r at the core–mantle boundary. Contour interval is 25 μT . Triangles show sites where data are available.

sites, or better distribution, or better averaging, etc.) for the N data. Values of -4° are reached only in West Africa and Hawaii, and again a large (-7°) anomaly centred on Indonesia is actually not locally constrained; 17 out of 31 sites have ΔI less than 2° . The inclination anomaly map for the R data appears much more rugged but actually, apart from China (8°), Hawaii (6°) and West Africa (7°), all sites show values less than $4-5^\circ$, often less than 3° . Declination anomalies are mostly less than 2° , and always less than 4° at all sites, except at the higher latitudes. We note in passing that there

is no evidence for large regional anomalies as have been hypothesized to explain some awkward palaeomagnetic data—for instance in Asia in the Tertiary by Westphal (1993).

It is clear that the simple (g_1^0, g_2^0) model could possibly be invalidated by more numerous, better distributed, or more accurate and representative data and complementary inversion techniques. The above results can be used to point out the directions in which it might next be desirable to go.

For one thing, the inverse technique of Johnson & Constable (1995) used throughout the present study makes simplifying

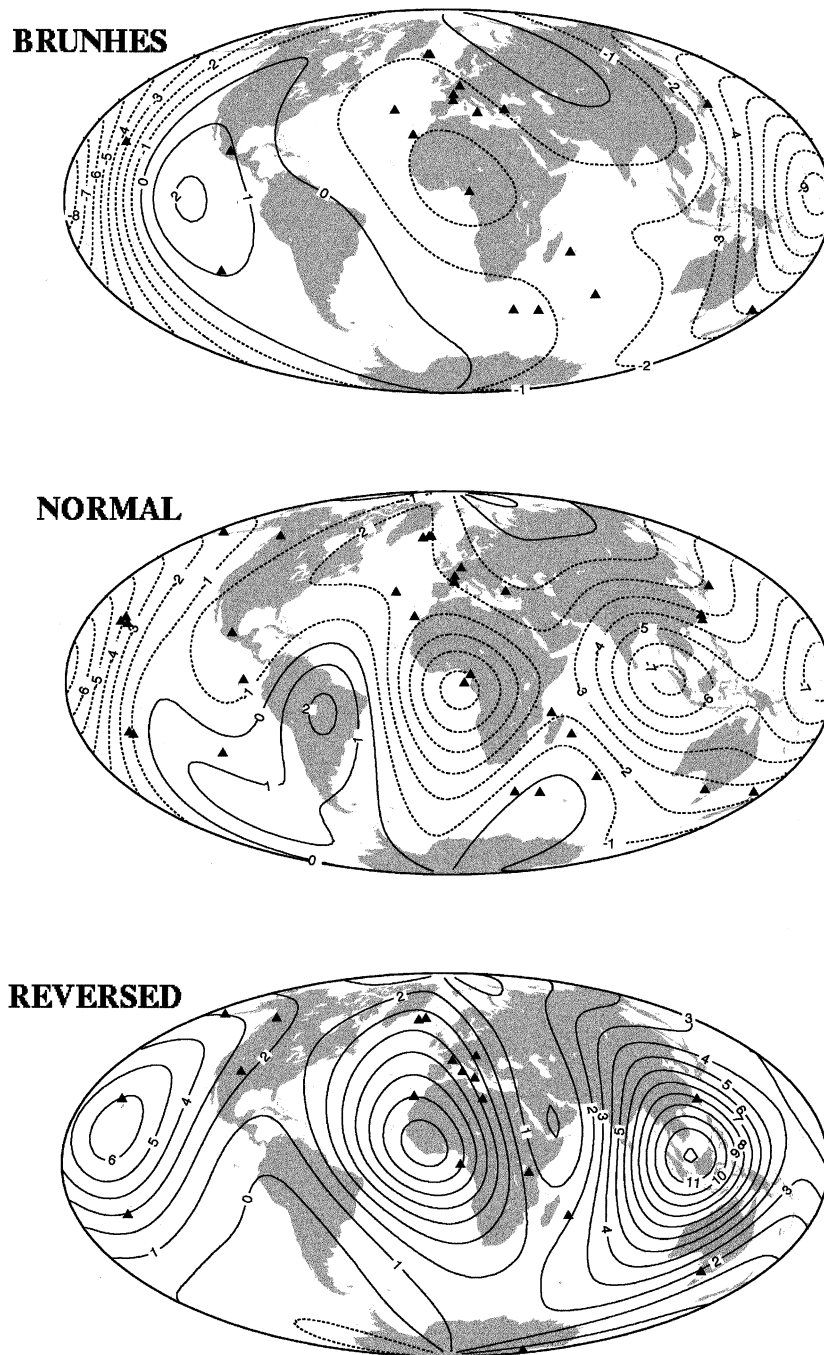


Figure 9. Maps of inclination anomalies (inclination corresponding to each field model from Fig. 8, minus inclination predicted for geocentric axial dipole), in degrees. Same format as Fig. 8.

assumptions as to the variance structure of the giant Gaussian process. Recent work, using various average distributions extracted from the data sets, has emphasized that, contrary to the hypotheses of Constable & Parker (1988, hereafter CP88), the variance of terms of a given degree may also depend on order. Quidelleur & Courtillot (1996) have shown that a larger value of σ_2^2 , the variance of the degree-2 and order-1 non-zonal quadrupole, was sufficient to account for much of the remaining misfit to the data set. Kono & Tanaka (1995b) and Hulot & Gallet (1996) have provided a theoretical basis to understand the importance of order $m = 1$ terms. Combining the distributions displayed by Quidelleur & Courtillot (1996)

with an inverse problem formulation based on theoretical descriptions and formulae of Kono & Tanaka (1995b) and Hulot & Gallet (1996) might allow one to go further and test the joint uncertainties of what appears today to be the most appealing and simplest model: a CP88-like giant Gaussian process with only one added free parameter (namely σ_2^2). It would remain to understand whether this new parameter actually provides information on the field generating process or remains an artefact due to data distribution.

Another predictive benefit of the inverse approach further discussed in this paper is to test how the situation could be improved by collecting more, better or other data. For instance,

one could test how acquisition of new PSV data from ill-sampled areas could alleviate some non-uniqueness. The geometry of the actual site distribution, this unavoidable spatial filter through which the core field must be viewed, is unlikely to change much in the near future. Indeed, this is a map of the main sources of abundant recent volcanism, mainly hot-spots, sufficiently remote from major tectonic disturbance. We have seen the major and adverse influence of sites such as Ethiopia, where tectonic rotations had not been properly assessed.

Clearly, new data from the central Pacific or southern Atlantic (e.g. Tristan da Cunha) would be extremely interesting. We should point out, however, that further sampling in areas where data are already available could be essential too. For instance, there are three sites within 50 km of each other in Reunion Island in the Indian Ocean that have yielded very discrepant inclination values of respectively $-38.9^\circ \pm 2.8^\circ$, $-29.1^\circ \pm 5.3^\circ$ and $-47.6^\circ \pm 1.6^\circ$ (uncertainties are σ_I calculated from the original data and augmented by 10 per cent as outlined in a previous section). Such values cannot be accounted for by the same low-order mean-field model. Problems linked to tectonics, palaeoslopes and incomplete removal of overprints could all have contributed, and further data from Reunion are clearly needed.

Vandamme *et al.* (1991) have shown, in the case of another large data set, that of lava flows from the Deccan traps in India, that improvement in palaeomagnetic techniques as time progressed was apparent in the data. Variances calculated with and without measurements made prior to 1980 were significantly different. Indeed, introduction of cryogenic magnetometers and better (and more systematic) magnetic cleaning and interpretation techniques for extracting primary magnetization directions make post-1980 data in general far more reliable. However, applying this criterion to the Q94 data set would reduce the number of data and site averages even further and make the inversion virtually impossible. For instance, selecting only those data involving proper cleaning and demagnetization (which implies rejection of undemagnetized NRM-only directions and blanket demagnetizations without vector diagrams) reduces the number of available, distinct sites in the Brunhes data from 20 to five! This clearly implies that inversion with data meeting now generally accepted quality criteria is still not possible. In any case, seriously underestimated published data uncertainties and various remaining sources of bias discussed in this paper underline the necessity of bringing detailed knowledge of what palaeomagnetic sampling, laboratory measurement and data interpretation actually amount to, into any long-term mean-field analysis. Once these have been sufficiently advanced, it will be useful to attempt to include sedimentary data and also palaeointensity data into the inversion. We believe, however, that the number and quality of much data and our understanding of whether they actually represent accurate pictures of the palaeofield at the kind of space and time resolution we are seeking for PSV analysis do not as yet allow them to be usefully incorporated into the PSV data set of lava flow palaeomagnetic directions. As pointed out above, a lot of homework (obtaining new directional data from both new and old sites) needs to be accumulated.

In conclusion, our belief is that available data do not require a more complex model than one in which the only non-zero spherical harmonic coefficients in the 1 to 5 Ma mean field are

the axial dipole and quadrupole. Asymmetries between the Northern and Southern Hemispheres, or between the normal and reversed states, are not yet resolvable. The most puzzling feature to be further analysed is the dependence of the variance of the various terms not only on degree but also on order, with the prominence of the order-1 quadrupolar variance.

NOTE ADDED IN PROOF

There has been since 1995 a healthy interaction between our group and the team formed by Catherine Johnson and Catherine Constable. The latest results of this are a set of two papers, the present one and a new one by Johnson & Constable (1997, hereafter JC97). The two papers were submitted to this journal respectively in December 1996 and January 1997. As might be expected, the senior authors were among the reviewers of the other's paper. Acceptance of JC97, and exchanges at the time of review, led us to this note added in proof in November 1997, which may be a useful complement to the main body of our paper.

The improvements and/or additions of JC97 over JC95 include the correction in the standard errors that was pointed out in Section 2.1. Also the lava data base is sifted and a number of data are eliminated on the basis of a number of potential problems and limitations. Data sets are averaged within 5° spatial bins. Finally, sediment data are included. JC97 use linearized data Green's kernels to demonstrate how declination and inclination data sample the core-mantle boundary; they argue that adding sediment to lava flow data improves CMB coverage.

In their new paper, JC97 reach a number of conclusions that differ from their JC95 views and come very close to our own results (see also Carlut & Courtillot 1995, 1996). JC97's new inverted models, like ours, incorporate a number of modifications and it is not always straightforward to evaluate the effects of single changes (data sifting, uncertainty modification, different data binning, inclusion of sedimentary data). But it is interesting that their final models are very significantly smoother than their JC95 results. When heavier smoothing constraints (norms) are used, the results are very similar to ours indeed. JC97 conclude, as we did, that much of the structure found in their previous models (JC95) can be attributed to sites with poor temporal sampling. Sediments (which, as stated above, we believe should probably not be used) are found not to contribute much structure. The high-latitude flux lobes are not observed, and JC97 conclude, like us, that they cannot be detected given the quality and distribution of current data sets.

The main feature on which we and JC97 would still differ is the significance of the non-zonal part of the field. The reality of a major anomalous feature in the Pacific Ocean would require further checking (it appears only when the maximum degree of the inversion is high—i.e. our Fig. 2b). But like us, JC97 now conclude that flux lobes in other models result from overprinting, that polarity asymmetries cannot be resolved, and that some of the data in existing databases need to be updated and complemented by further work: in other words, a number of data are probably affected by significant undetected errors, and proper palaeomagnetic analysis of each datum is required (and often not even sufficient to uncover the sources of anomalies).

We also wish to point the reader's attention to another paper that appeared after ours was submitted (Kelly &

Gubbins 1997). This is a development on the earlier Gubbins & Kelly (1993) paper, though there are still problems, which are adequately addressed by JC97 and need not be repeated here.

ACKNOWLEDGMENTS

We thank Catherine Constable for an extensive review of the manuscript. We are also grateful to Phillip McFadden and Michael McElhinny for their comments on an early version. IGP contribution 1540.

REFERENCES

- Bloxham, J. & Gubbins, D., 1985. The secular variation of the Earth's main magnetic field, *Nature*, **317**, 777–781.
- Bloxham, J. & Jackson, A., 1992. Time-dependent mapping of the magnetic field at the core–mantle boundary, *J. geophys. Res.*, **97**, 19 537–19 563.
- Carlut, J. & Courtillot, V., 1995. Geomagnetic paleosecular variation in the last 5 million years: How many multipoles are actually resolvable? (abstract), *EOS Suppl.*, **76** (46), 166 (Nov. 7).
- Carlut, J. & Courtillot, V., 1996. How complex is the Earth's average magnetic field? (abstract), *EOS Suppl.*, **77** (22), 143 (May 28).
- Constable, C.G. & Parker, R.L., 1988. Statistics of the geomagnetic secular variation for the past 5 Myr, *J. geophys. Res.*, **93**, 11 569–11 581.
- Constable, S., Parker, R. & Constable, C., 1987. Occam's inversion: a practical algorithm for generating smooth models from electromagnetic sounding data, *Geophysics*, **52**, 289–300.
- Courtillot, V., 1980. Opening of the Gulf of Aden and Afar by progressive tearing, *Phys. Earth planet. Inter.*, **21**, 343–350.
- Courtillot, V. & Valet, J.-P., 1995. Secular variation of the Earth's magnetic field: from jerks to reversals, *C.R. Acad. Sci. Paris*, **320**, 903–922.
- Courtillot, V., Achache, J., Landre, F., Bonhommet, N., Montigny, R. & Féraud, G., 1994. Episodic spreading and rift propagation: new paleomagnetic and geochronologic data from the Afar nascent passive margin, *J. geophys. Res.*, **99**, 3315–3333.
- Courtillot, V., Valet, J.-P., Hulot, G. & Le Mouél, J.-L., 1992. The Earth's magnetic field: Which geometry? *EOS, Trans. Am. geophys. Un.*, **73**, 337 and 340–342.
- Gubbins, D. & Kelly, P., 1993. Persistent patterns in the geomagnetic field over the past 2.5 Myr, *Nature*, **365**, 829–832.
- Hulot, G. & Gallet, Y., 1996. On the interpretation of virtual geomagnetic pole (VGP) scatter curves, *Phys. Earth planet. Inter.*, **95**, 37–53.
- Hulot, G. & Le Mouél, J.-L., 1994. A statistical approach to the Earth's main magnetic field, *Phys. Earth planet. Inter.*, **82**, 167–183.
- Hulot, G., Khokhlov, A. & Le Mouél, J.-L., 1997. Uniqueness of mainly dipolar magnetic fields recovered from directional data, *Geophys. J. Int.*, **129**, 347–354.
- Johnson, C. & Constable, C., 1995. The time-averaged field as recorded by lava flows over the past 5 Myr, *Geophys. J. Int.*, **122**, 489–519 (JC95).
- Johnson, C. & Constable, C., 1996. Paleosecular variation recorded by lava flows over the last 5 Myr, *Phil. Trans. R. Soc. Lond.*, **354**, 89–141 (JC96).
- Johnson, C. & Constable, C., 1997. The time-averaged geomagnetic field: global and regional biases for 0–5 Ma, *Geophys. J. Int.*, **131**, 643–666 (JC97).
- Kelly, P. & Gubbins, D., 1997. The geomagnetic field over the past 5 million years, *Geophys. J. Int.*, **128**, 1–16.
- Kono, M. & Tanaka, H., 1995a. Intensity of the geomagnetic field in geological time: a statistical study, in *The Earth's Central Part: Its Structure and Dynamics*, pp. 75–94, ed. Yukutake, T., Terrapub, Tokyo.

- Kono, M. & Tanaka, H., 1995b. Mapping the Gauss coefficients to the pole and the models of paleosecular variation, *J. Geomag. Geoelectr.*, **47**, 115–130.
- Lee, S., 1983. A study of the time-averaged paleomagnetic field for the last 195 million years, *PhD thesis*, Australian National University, Canberra.
- Loves, F.J., 1974. Spatial power spectrum of the main geomagnetic field and extrapolation to the core, *Geophys. J. R. astr. Soc.*, **36**, 717–730.
- Manighetti, I., 1993. Dynamique des systèmes extensifs, *PhD thesis*, IGP, Paris.
- Manighetti, I., Tapponnier, P., Courtillot, V. & Gruszow, S., 1997. Propagation of the Arabia–Somalia boundary: I—The Gulfs of Aden and Tadjoura, *J. geophys. Res.*, **102**, 2681–2710.
- McElhinny, M.W., McFadden, P.L. & Merrill, R.T., 1996. The time-averaged paleomagnetic field 0.5 Ma, *J. geophys. Res.*, **101**, 25 007–25 027.
- Merrill, R. & McElhinny, M., 1977. Anomalies in the time-averaged paleomagnetic field and their implications for the lower mantle, *Rev. Geophys.*, **15**, 309–323.
- Merrill, R. & McElhinny, M., 1983. *The Earth's Magnetic Field*, Academic Press, London.
- Quidelleur, X. & Courtillot, V., 1996. On low-degree spherical harmonic models of paleosecular variation, *Phys. Earth planet. Inter.*, **95**, 55–77.
- Quidelleur, X., Valet, J.-P., Courtillot, V. & Hulot, G., 1994. Long-term geometry of the geomagnetic field for the last five million years: an updated secular variation database, *Geophys. Res. Lett.*, **15**, 1639–1642 (Q94).
- Schneider, D. & Kent, D., 1988. The paleomagnetic field from equatorial deep-sea sediments: axial symmetry and polarity asymmetry, *Science*, **242**, 252–256.
- Schult, A., 1974. Paleomagnetism of Tertiary volcanic rocks from the Ethiopian southern plateau and the Danakil block, *J. Geophys.*, **40**, 203–212.
- Tanaka, H., Turner, G.M., Houghton, B.F., Tachibana, T., Kono, M. & McWilliams, M.O., 1996. Palaeomagnetism and chronology of the central Taupo Volcanic Zone, New Zealand, *Geophys. J. Int.*, **124**, 919–934.
- Tapponnier, P., Armijo, R., Manighetti, I. & Courtillot, V., 1990. Bookshelf faulting and horizontal block rotations between overlapping rifts in southern Afar, *Geophys. Res. Lett.*, **17**, 1–4.
- Tarling, D.H., 1983. *Paleomagnetism: Principles and Applications in Geology, Geophysics and Archeology*, Chapman and Hall, London.
- Vandamme, D., Courtillot, V., Besse, J. & Montigny, R., 1991. Paleomagnetism and age determinations of the Deccan traps (India): results of Nagpur–Bombay traverse and review of earlier work, *Rev. Geophys.*, **32**, 61–83.
- Westphal, M., 1993. Did a large departure from the geocentric axial dipole hypothesis occur during the Eocene? Evidence from the magnetic polar wander path of Eurasia, *Earth planet. Sci. Lett.*, **117**, 15–28.
- Wilson, R.L., 1970. Permanent aspects of the Earth's non-dipole magnetic field over upper Tertiary times, *Geophys. J. R. astr. Soc.*, **19**, 417–437.
- Wilson, R.L., 1971. Dipole offset: the time-averaged paleomagnetic field over the past 25 million years, *Geophys. J. R. astr. Soc.*, **22**, 491–504.

APPENDIX A: THE DATA SETS

We briefly recall the reference and/or definition of a number of data sets, and subsets or modifications thereof, which are used in this paper. They are listed under the code used to refer to them in the paper.

- (1) *JC96*: The data set introduced by Johnson & Constable

(1996) and used in Johnson & Constable (1995) to calculate average field models. The subset used to produce model LB1 is labelled JC96-1, and that used to produce a smoother model LB2, after removal of four anomalous sites, is labelled JC96-2.

(2) *Q94*: The data set introduced by Quidelleur *et al.* (1994). Among several criteria, similar to those used in other studies (Lee 1983; Johnson & Constable 1996), Quidelleur *et al.* included quantitative criteria to eliminate single sites in which secular variation had not been averaged out, namely those in which the precision parameter exceeded 85 (indicating very large correlation between flow directions, because of either too few flows or too little time between flows). This involved eight sites in the Indian Ocean, western Pacific, Yellowstone, Hawaii, Kauai, Ethiopia, Niihau and Norfolk Island.

(3) *Q94-m*: *Q94* modified with more selective criteria: (a) at least four samples per flow (three in JC96 and two in *Q94*); (b) at least eight flows per site (five in JC96 and in *Q94*); (c) transitional directions, i.e. with the absolute value of virtual

geomagnetic pole (VGP) latitude less than 55° (45° for *Q94*) rejected; (d) all sites within a 1° geographical 'square' grouped together.

(4) *Q94-me*: This is *Q94-m* with the data from Ethiopia (Schult 1974) removed. Altogether, this data set contains directional averages from 31 normal and 19 reversed sites (or supersites). As illustrated in this and earlier papers, large geographical areas are still devoid of data.

(5) We have made a new updated set available on the IGP web site in 1997 (<http://www.ipgp.jussieu.fr/depts/PALEOMAG/VARSECU/Introbrit.html>). This was not used in the present paper, which was based on the earlier version *Q94* and derivations. Note also that another base will shortly be available from M. McElhinny (personal communication, 1997). These are all particularly welcome, as this paper hopefully demonstrates the importance of checking field models against all possible subsets and versions of directional PSV data sets.